Global NEST Journal, Vol 27, No 1, 06360

Utilizing industrial by-products in autoclaved aerated concrete: A sustainable approach

Jagadheeswari R.[1*] and Sumathy S.R.[2]
1*Department of Civil Engineering, K Ramakrishnan College of Technology, Trichy - 621112, Tamilnadu, India
[2]Department of Civil Engineering, Alagappa Chettiar Government College of Engineering and Technology, Karaikudi - 630003, Tamilnadu, India
Received: 02/07/2024, Accepted: 02/11/2024, Available online: 25/11/2024
*to whom all correspondence should be addressed: e-mail: sivag616@gmail.com
https://doi.org/10.30955/gnj.06360

Graphical abstract

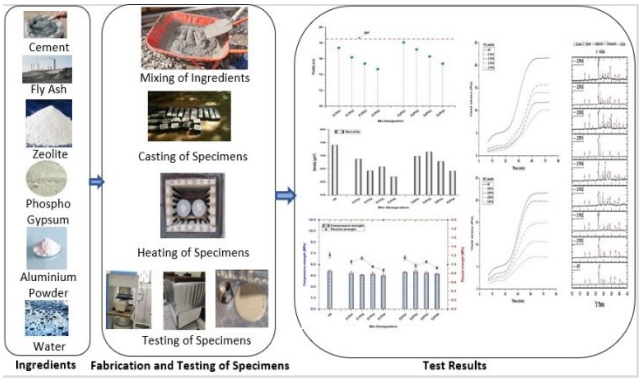

Abstract

The feasibility of utilizing natural zeolite (NZ), phosphogypsum (PG), and aluminium (Al) powder (AP) as replacements for fly ash in autoclaved aerated concrete (AAC) is assessed in this research. This study examines the influence of NZ, PG and AP on AAC's fresh state properties, mechanical behavior, and thermal characteristics. Gas foaming properties were analyzed using X-ray diffraction (XRD) and Fourier Transform Infrared Spectroscopy (FTIR). Results show that natural zeolite and aluminum powder have acceptable foaming properties that contribute to AAC's porosity and lightness when combined with phosphogypsum. The optimal dosage of PG, along with 10% and 20% zeolite and aluminum powder, enhances AAC performance through a synergistic effect. PG substitution for fly ash reduced density and increased the pH of the AAC slurry, affecting foam generation. Incorporation of PG potentially reduced workability due to its smaller particle size and larger surface area. Despite this, NZ, PG, and AP combinations resulted in AAC with satisfactory strength and flexural properties. AAC with phosphogypsum showed good strength, density, and thermal conductivity, though thermal conductivity was highest in control AAC. This study demonstrates these materials' potential to meet AAC's construction requirements economically and efficiently dispose of phosphogypsum. Future research should explore other material combinations and their impacts on AAC, supporting sustainable construction and resource management.

Keywords: AAC, natural zeolite, phosphogypsum, aluminium powder, strength, foaming property, microstructure

1. Introduction

Buildings' total carbon emissions and energy use during their lifetimes are rising due to urbanisation (González *et al*., 2022). Greenhouse gas emissions can be lowered and the environment protected with the help of energy-efficient construction. It is crucial to advance and popularise carbon-neutral and energy-efficient construction supplies. AAC has more potential for use in the background of universal efforts to encourage construction energy savings and decrease carbon dioxide emissions. Recently, interest has risen in the use and improvement of insulating materials for buildings that condense energy utilization (Tian *et al*., 2016; Yang *et al*., 2021; Falliano *et al*., 2022). Autoclaved aerated concrete (AAC) is a lightweight, porous construction element that can bear significant loads and offers superior insulating properties. AAC has been suggested as a means of improving energy efficiency (Kadhim *et al*., 2020; Wang *et al*., 2021) could be a possible solution, and the product reveals small bulk density, good thermal insulation and fire resistance, which can be possibly applied in non-load-bearing structures and as thermal insulation materials for walls in buildings (Trindade *et al*., 2021; Xu *et al*. 2021; Qian and Hu 2023). Due to their beneficial effects on efficiently harnessing seismic loads, lightweight materials have seen widespread application in recent years (Seddighi *et al*., 2021). Its density can range from 300 to 1800 kg/m^3 but is typically 400 to 600 kg/m^3 (Zhai *et al*., 2018). Its structure comprises 60-80% non-connected air pores, which are liable to the density class. Typically, siliceous materials like quartz powder or fly ash and calcareous raw materials like lime and cement, laterally with supplements like foaming agents and water, are

autoclaved at temperatures considerably more significant than 100°C in a pressurised, steam-heated environment to create AAC (Schreiner *et al*., 2018; Natarajan *et al*., 2021). Acquiring insulating materials for strong and lightweight buildings has always been an objective and a course of action.

For this reason, the sector's goal has been extended to produce AAC with greater compressive strength within a given range of density oscillation. Due to its high porosity, the pore structure is a significant determinant of AAC's dry density and compressive strength. Pore structure analysis has emerged as a fundamental topic in concrete materials science (Kumar *et al*., 2024). AAC's pore structure is comprised mainly of the porosity, number of holes, average pore size, and hole shape component of its pores (Zhang *et al*., 2023). The mechanical attributes of cement-based materials are closely related to their degree of porosity (Revilla *et al*., 2021; Loginova *et al*., 2023). As the porosity of AAC increases, its compressive strength drops dramatically (He *et al*., 2019). Improved indoor comfort is possible thanks to AAC due to the material's porous properties, high heat preservation, and sound insulation abilities (Qu and Zhao 2017; Liu *et al*., 2020). The trend has shifted even more towards using industrial by-products to make high-performance AAC. This refers to AAC that maintains its volume, is mechanically robust, and provides excellent thermal insulation (El-Didamony *et al*., 2019). The fact that fly ash, iron tailings, zinc tailings, and sludge can all be utilised in the production of AAC demonstrates a significant opportunity for improving the current rate of solid waste utilisation (Serhat *et al*., 2014; Walczak *et al*., 2015; Suchorab *et al*., 2016; Miao *et al*., 2023). Solid wastes made AAC, including calcium carbide slag, gold tailings, and silica fume (Cai *et al*., 2018; Li *et al*., 2019; Zhao *et al*., 2020). This strategy can considerably reduce the price of finished products while still being environmentally friendly and sustainable (Guo and Zhang, 2020). Cementitious materials, such as siliceous and calcareous, comprise the bulk of AAC's raw materials. Classic examples of siliceous minerals include quartz sand and silica sand, which typically have SiO_2 concentrations above 90%.

AAC's thermal insulation qualities are superior to regular concrete's, and its density is significantly lower (Ma *et al*., 2016; Yuan *et al*., 2017; Asadi *et al*., 2018). The economic viability of AAC products is constrained by characteristics such as their fragility and lack of mechanical strength (Koudelka *et al*., 2015; Cong *et al*., 2016; Johnson *et al*., 2021). AAC's widespread application in buildings may be traced back to the rise of the "carbon neutralisation" development aim in recent years, which many countries have suggested. Insufficient mechanical characteristics, especially flexure, have been identified as a significant source of AAC non-compliance through preceding investigations publicizing that breakage, cracking, and frost failure are expected during the manufacturing, transportation, and service phases of AAC products (Huang *et al*., 2022). While cement hydration releases calcium hydroxide, adding aluminium powder to cement-based products stimulates a chemical interaction between the powder and water, producing hydrogen gas and forming porous interior structures (Ahmed *et al*., 2024). The aluminium powder-cement paste chemical reaction is shown as: (Singh *et al*., 2020; Wang *et al*., 2023)

$$2Al + 3Ca(OH)_2 + 6H_2O = 3CaO.Al_2O_3.6H_2O + 3H_2 \uparrow$$

Cellular holes between 0.1 and 1.0 mm in size have been reported to be produced in the literature during this chemical process. Consequently, cement-based products with a density of 300-1,800 kg/m^3 can be made significantly lighter by adding aluminium powder (Ahmed *et al*., 2022). Because of this, there have been a lot of inquiries to emphasise the crucial role that aluminium particles' integration into an insulating polymer plays in enhancing the material's mechanical, tribological, thermal, and electrical properties (Zhang *et al*., 2022). Mechanical, tribological, and electric properties of mixtures were investigated after a novel composite material was produced by filling aluminium powder in acrylonitrile butadiene styrene. A larger powder loading of aluminium filler was shown to have a pronounced effect on the impact, tensile, and flexure of the matrix, as demonstrated by their experiments (Laad and Jatti 2015). A different investigation found that ageing aluminium powder composites improved their resistance to heat, ozone, and gamma radiation. To properly understand cement-based materials ' features that combine pore formation components, it's essential to conduct more microscale research to analyse the connection between porous structures and hardened properties. Very porous cement-based materials' mechanical characteristics and longevity are subpar (Li *et al*., 2015; Kim *et al*., 2018).

Industrial waste material phosphogypsum (PG) is produced during the wet production of phosphoric acid. For every ton of phosphoric acid produced, about 5 tons of PG are by-products (Rashad 2017). Approximately 85 percent of all PG is frequently discarded in gigantic mounds without being handled. This leaves it vulnerable to occupying a large amount of land through the progression of weathering and inflicting substantial damage to the natural world, especially along the coast (Zhao *et al*., 2023). Consequently, several nations have studied PG disposal alternatives in response to widespread resentment. An alternative to the location where waste is disposed of can be achieved by using PG as a binder in civil building activities (Qiao *et al*., 2020). Recently, much emphasis has been placed on PG's potential as a versatile raw material in the food industry. In the cement industry, PG has been employed as a setting regulator instead of natural gypsum, paving an efficient way to save money (Li *et al*., 2020). The practice of natural gypsum in setting regulator applications has been replaced mainly by using PG in the cement and gypsum industries. Because of radioactive concerns, PG is not widely adopted in the building business. However, this problem may be overcome by limiting the quantity of PG included in building materials. According to the studies, this would result in radioactivity control that was entirely

risk-free for the construction industry (Campos *et al*., 2017). Because of the rising amount of garbage being produced, it is imperative that these waste materials, in addition to PG, be put to use to prevent the rapid deterioration of the environment (Chen *et al*., 2021). Ordinary Portland cement, oilwell cement, calcium sulfoaluminate cement, and magnesium phosphate cement are some of the types of cement that make extensive use of PG (Aminul *et al*., 2020; Mohammadi *et al*., 2020; Rosales *et al*. 2020; Reddy *et al*., 2022; Nambiar *et al*., 2023). Impurities soluble in phosphoric acid can extend the time needed for the setting process and lower the water-to-binder ratio (Holanda *et al*., 2017). These impurities have the potential to transform into phases that are insoluble in some types of cement that have a high aluminium content.

Zeolite, a naturally occurring aluminosilicate, offers unique properties that enhance the performance of AAC. Its high silica and alumina content makes it a suitable replacement for traditional binders like fly ash, contributing to the pozzolanic reaction, which enhances the strength and durability of AAC. Additionally, zeolite's porous structure improves the thermal insulation properties of AAC, making it an ideal candidate for energy-efficient building materials (Rahman *et al*., 2021). Studies have shown that the inclusion of natural zeolite in concrete mixtures can lead to improved compressive strength and long-term stability, as well as reduced autoclaving time due to accelerated hydration processes (Shekarchi *et al*., 2023). Moreover, the environmental benefits of using zeolite in AAC are considerable. By reducing the reliance on energy-intensive materials like Portland cement, the carbon footprint of AAC production is lowered, aligning with sustainable construction practices. Zeolite's ability to absorb and neutralize harmful chemicals also adds to its eco-friendly profile, making AAC with zeolite a promising material for future green building projects (Alexa-Stratulat *et al*, 2023).2. Research Significance

Although it has been shown through a series of tests that aluminium powder may be carried out to form porous structures in cement-based materials, the outcomes of mixing the two materials and lags in defining the mechanism of their interface, this study focused on the exploitation of phosphogypsum, aluminium powder, and natural zeolite together to develop a better, more durable, and lighter-weight concrete. Regarding the manufacturing of AAC, the aerating agent is the most expensive component. Pure aluminium (Al) powder is the preferred aerating agent for this application's production of lightweight AAC. The primary goal was to determine whether or not the addition of natural zeolite and phosphogypsum could be employed to produce AAC that exhibited higher mechanical performance. When making AAC for testing purposes, different proportions of phosphogypsum and two standard concentrations of zeolite (10% and 20%, respectively) were added to the mixes by the ratios of commercially available AAC.

2. Experimental programs

2.1. Materials

Cement, fly ash, zeolite, lime, phosphogypsum, and aluminium powder were all purchased from Astrra Chemicals in Tamil Nadu, India, to prepare AAC samples. Each ingredient is essentially intended to create AAC and satisfy the necessary standards. Ordinary Portland cement with a grade of 53 is the type of cement employed in manufacturing concrete mixes. According to IS code 12269-1987, the fineness of the cement shall be more excellent than 225 m^2/kg, and the soundness should be at least 10 mm and 0.8% for Le Chatellier expansion and Autoclave expansion, respectively. In addition, aluminium powder is utilized as the expanding agent to increase the slurry's capacity while lowering its density. **Table 1** presents the oxide composition of the raw materials as tested in lab, while **Figure 1** illustrates their particle size distribution curves.

Table 1. Percentage of Oxide composition of raw materials

Composition	Cement	Lime	Flyash	NZ	PG	AP
SiO_2	26.01	1.2	58.22	63.87	3.66	0.1
CaO	53.6	89.1	3.28	2.37	32.31	0.1
SO_3	2.77	2.2	0.28	-	41.94	-
Al / Al_2O_3	8.54	0.4	28.31	11.47	0.23	99.5
MgO	0.35	0.7	1.14	1.01	0.03	0.1
MnO	0.13	-	-	-	-	-
K_2O	0.9	0.1	0.41	0.94	0.02	-
TiO_2	0.42	-	1.01	-	-	-
P_2O_5	0.17	-	-	-	0.45	-
Na_2O	0.18	1.1	0.62	6.81	0.02	0.1
Fe_2O_3	4.09	0.3	3.76	0.22	0.2	0.1
LOI	2.7	3.7	2.97	11.97	21.14	-

2.2. Sample preparation

In this experiment, the constituents used were lime, cement, fly ash, zeolite, phosphogypsum, and water. The ratios of cement, lime, aluminum powder, and water were kept constant during the mixing process. The mixture has been finely pulverized, and the slurries have been mixed at room temperature for sixty seconds. Then, the slurry was blended with aluminium powder while stirred for

thirty seconds. Slurries were poured into steel moulds of various sizes (100 mm by 100 mm by 100 mm) and then maintained in a steam curing chamber with a continuous temperature of 600 °C to finish the curing process. After removing the portion that had expanded out of the steel mould, demold the remaining material to obtain samples with dimensions of 100 millimetres on each side, 100 millimetres in length, and 100 millimetres in height.

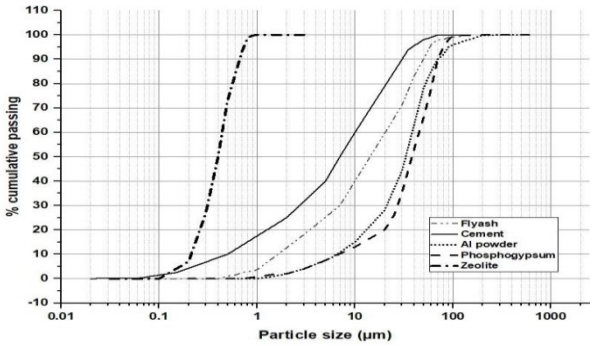

Figure 1. PSD curves of raw materials

At last, the sample that has been demoulded is placed inside an autoclave for eight hours at a temperature of 2,000 degrees Celsius and a pressure of two megapascals. Samples were prepared to assess the impact of various replacements on the characteristics of slurry and AAC. Phosphogypsum was used in place of fly ash at percentages of 0%, 5%, 10%, 15%, and 20% by weight, respectively. In addition, a consistent cement substitution of 10% to 20% zeolite is utilized across the board in all mixes. Powdered aluminium is added in an amount equal to 0.5% of the overall mass of the binder. The goal of the Z1PG1–Z1PG4 samples was to see how different amounts of PG affected the AAC's functional characteristics. In contrast, the Z2PG1–Z2PG4 samples contained 20% zeolite as a consistent replacement. No alternatives exist in the reference mix (RF), such as zeolite and phosphogypsum. **Table 2** displays the mix proportions and the water-solid ratio (w/s). The selection of component ranges in **Table 2** was based on a combination of preliminary experiments, previous literature, and the need to maintain optimal properties of the concrete mix. Specifically, the maximum inclusion of phosphogypsum was limited to 20%, to avoid potential adverse effects on compressive strength and workability, which can occur at higher concentrations. Studies have shown that higher ratios of phosphogypsum can negatively impact the mechanical properties of concrete (Arunprathap *et al*., 2020; Murali & Azab, 2023).

2.3. Characterizations and tests

2.3.1. Raw materials

To identify the individual chemical components of raw materials, an X-ray fluorescence (XRF) analyzer was utilized. Quantification was done on the particle size distributions of cement, fly ash, zeolite, powdered graphite, and powdered aluminium.

2.3.2. Properties of slurry

The gas-foaming rate was determined by monitoring the slurry volume measurement in a measuring cylinder that had a capacity of 250 ml and had been stuffed with 100 ml of initial slurry once every 10 minutes until the slurry stopped growing in volume. The readings of PG's pH were determined as per ASTM C471M-20, and the pH/ion meter was used to develop the determinations. Before conducting the tests, powder samples were made in agreement with **Table 2** (but without adding Al powder or water). The slurry was finally ready for use after thoroughly combining the powder samples and water for ten minutes at a w/s ratio of 0.55. After filtering the slurry to acquire the filtrate liquid, a pH test was carried out on the product of the extraction of liquid from the filtering process.

Table 2. Mix proportion of developed samples

Mix Id	Cement in %	Lime in %	Flyash in %	Zeolite in %	Phospho-gypsum in %	Al powder in %	w/s
RF	10	15	75	0	0	0.5	0.55
Z1PG1	10	15	60	10	5	0.5	
Z1PG2	10	15	55	10	10	0.5	
Z1PG3	10	15	50	10	15	0.5	
Z1PG4	10	15	45	10	20	0.5	
Z2PG1	10	15	50	20	5	0.5	
Z2PG2	10	15	45	20	10	0.5	
Z2PG3	10	15	40	20	15	0.5	
Z2PG4	10	15	35	20	20	0.5	

2.3.3. Fresh state

First, the paste was put into the mould until it reached a height equal to two-thirds of the height of the mould, and then the mould was tamped 15 times. Next, the paste was poured into the mould until it reached a height 20 millimetres higher than the mould, which was tamped ten more times. Following the completion of the tamping process, the formwork was removed. The yield stress was calculated through a rheometer at a temperature of 27±20°C. One millilitre of freshly made AAC paste was placed between two parallel titanium plates with a diameter of 35 mm and a spacing of 1.1 mm. During the first minute of the experiment, a constant shear rate of 0.5 s^{-1} was applied to the paste to overcome the initial inertia of the rheometer and break up any agglomerations that had formed due to the hydration process. Following this, the shear rate decreased linearly from 0.5 to 0.08 s^{-1} over three minutes, with a reduction step of 0.004 s^{-1}, the smallest measurable value using the rheometer. According to Pinilla *et al*. (2014), the rheological behaviour

of aerated cement paste can be modelled using the Bingham model. According to the Bingham model, the equation that describes the relationship between shear stress and shear rate is as follows:

$$\tau = \tau_0 + \mu \quad (1)$$

Where τ_o and μ represent the yield stress and viscosity of the fresh paste, respectively, Equation (2) was used to predict the yield stress of the AAC pastes by fitting it to the experimental data obtained from the a vs. curve. To determine the volume expansion capacity of the AAC, 40 ml of fresh AAC paste was poured into a 100 ml measuring cylinder and stored in an environmental chamber at the same pre-curing temperature and relative humidity as the AAC cube samples. These conditions were 550 degrees Fahrenheit and 98% relative humidity. Every five minutes, the size of the paste was measured and recorded until there was no longer any change. The following equation was used to calculate the volume expansion, denoted by V_t (in ml) at time t:

$$\Delta V_t = V_t - V_0 \quad (2)$$

Where V_t is the paste volume at time t in ml, and V_0 is the initial paste volume (40 ml). It is vital to remember that the measurement method, particularly the mould's base area chosen to estimate the volume expansion capacity, might have a consequence on the results.

2.3.4. Mechanical behavior of AAC

The ASTM C1693-11 standard measured the AAC samples' bulk densities. For compressive and flexural strength tests, specimens with overall dimensions of 100 mm x 100 mm x 100 mm and 50 mm x 50 mm x 200 mm were constructed. The samples were put into an oven preheated to 600 degrees Celsius for one full day to condition them. Afterwards, they were detached from the oven and allowed to relax for 120 minutes before the tests. Evaluation was done on three samples of each composition and pure AAC.

2.3.5. Thermal conductivity

The developed slurry was set into the mould with dimensions of 70.7 mm by 70.7 mm by 70.7 mm, and the extra part that extended beyond the part of the mould where it was supposed to be was chopped off. After the cubes were obtained, they were positioned in the autoclave to undergo the curing process. After the time in the autoclave had elapsed, the cubes were removed and baked at 105 degrees Celsius for three days.

2.3.6. Microstructural characterization

X-ray diffraction was utilized as the analysis method to study the crystalline phases present in AAC. The XRD tests were executed with the assistance of an XPert Pro PANalytical diffractometer, and the patterns were captured at two different angles. FTIR examinations were carried out to obtain the spectral curves of AACs. The curves were acquired using the Shimadzu IR Tracer apparatus at a wavelength ranging from 400 to 4500 cm^{-1} utilizing the KBr pellet approach. After the AAC samples were ground into a powder, about one milligram of the powdered AAC samples was combined with 99% potassium bromide (kBr). After that, the mixture is pelletized by creating a homogenous mixture, which leads to the development of crystalline pellets with a hazy appearance.

3. Results and discussions

3.1. Fresh state behaviour

3.1.1. Fluidity

The fluidity of the slurry defines the expansion behaviour and gas foaming capacity of the AAC mixes. This is accomplished through the uniform development of pores in the AAC. As shown in **Figure 2**, the fluidity of the AAC mixes became less manageable as the proportion of existing PG additives in the mixture increased. It is readily apparent that the control AAC can achieve better workability. It was revealed that the fluidity of the AAC mix, including 10% New Zealand wool and 20% polypropylene glycol, was 20.5% less than the fluidity of the control mix, indicating that the viscosity of the AAC mixes had grown.

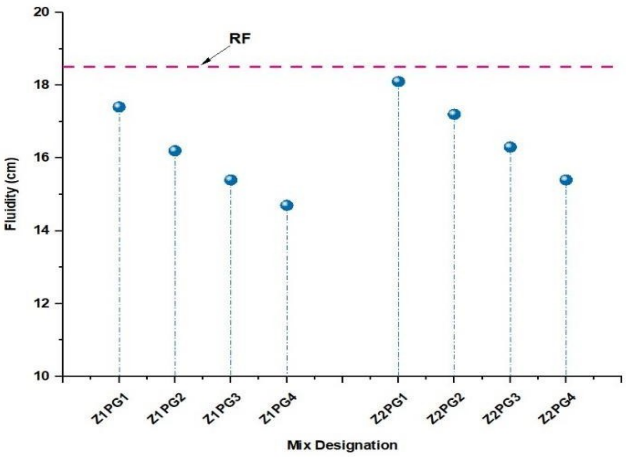

Figure 2. Effects of PG and NZ contents on the slurry fluidity of AAC

Additionally, the fluidity of the AAC mix containing 20% New Zealand wool and the same percentage of PG was reduced by 16.8%. Because of its higher surface area and porous structure, NZ with PG requires more water, significantly reducing its workability. However, the thickening behaviour of the NZ when combined with PG was prolonged, which led to a broader time space for the growth of a greater quantity of gas pores.

3.1.2. Yield stress development

Figure 3 illustrates the progression of yield stress over time for the AACs examined in a specific study. It shows that after 60 minutes; the yield stress begins to stabilize. This finding supports that yield stress measurements were only conducted for 70 minutes in this study, aligning with the average initial setting time of OPC, which is also 60 minutes. The production of hydration products caused the yield stress to increase over time for all AACs; however, the rate of increase varied for each AAC. This variation occurred because, during the initial stages of hydration, the AAC paste containing 20% PG exhibited the lowest

yield stress, followed by 15%, 10%, and 5% PG, respectively, when 10% NZ was substituted for fly ash. The highest yield stress was in the AAC paste containing 5% PG. Scientists have found that adding more PG to the AAC commanded a decrease in yield stress experienced at both 10% and 20% NZ. This is chiefly owing to the creation of a porous microstructure with a more significant percentage of PG, which absorbs more water. Because the control AAC has less freely available water, the yield stress of the fresh paste is increased.

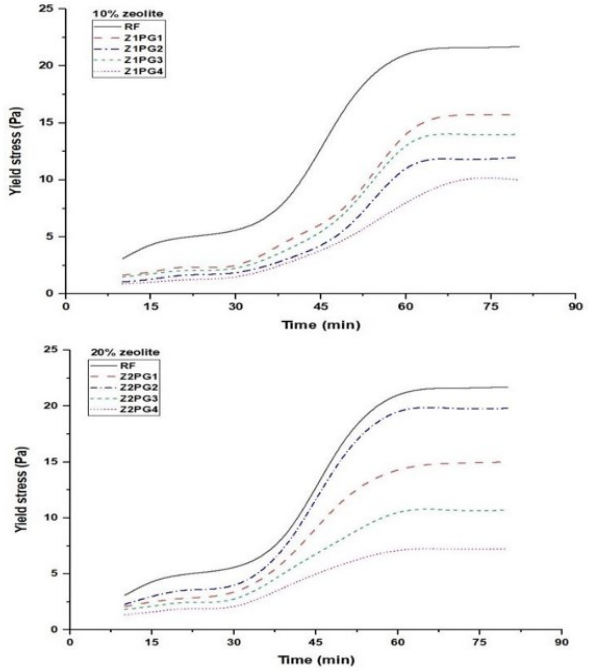

Figure 3. Yield stress vs time of developed AACs

3.1.3. Volume expansion of AAC

Figure 4 depicts the fresh AAC pastes' expansion of volume over time. The increase in total volume during AAC can be divided into four distinct phases: the induction stage, the acceleration stage, the deceleration stage, and the steady-state stage. During the induction period of the aeration process, the fresh paste retains nearly all of its initial volume following the mixing stage. During this time, there has also been very little expansion. The creation of a passivation deposit (made of aluminium oxide) on the exterior of the aluminium particles is what causes the induction period. This layer prevents the gas generation reaction from occurring during the allotted time. At this point, the passivation layer is eroded by hydroxyl radicals, which are created by the reaction of aluminium oxide with water. The second stage is known as the acceleration period, and there has been a notable increase in the volume of the fresh paste. This happens since the paste is under low yield stress, and the aeration process is chemically controlled. The deceleration stage is marked by a reduction in the volume expansion rate, even though the volume of the fresh paste continues to increase. At this stage, the yield stress of the paste rises, leading to reduced aeration. In the final phase, called the steady state, the volume expansion of the fresh paste ceases as the paste continues to stiffen. The duration of each stage in the process is influenced by the fresh paste's rheological properties and the aerating agent's gas production potential over time.

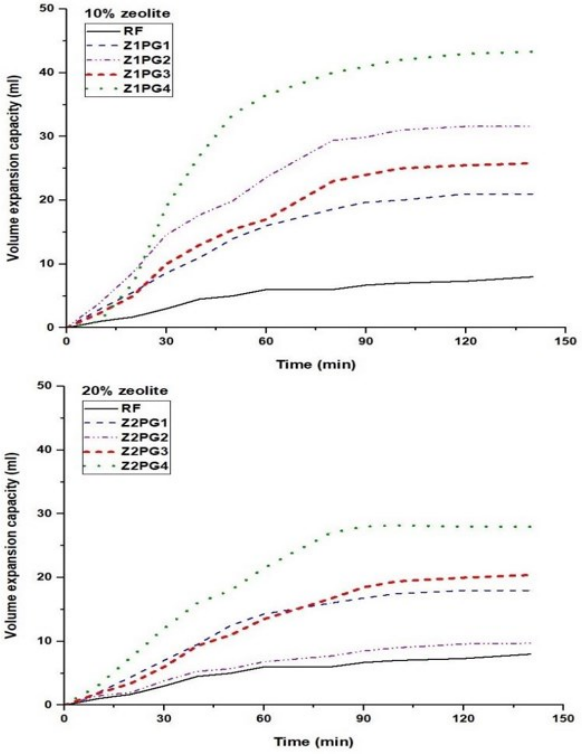

Figure 4. Volume expansion capacity of developed AACs

At the culmination of the 140-minute test, the 20% PG-substituted AAC with 10% and 20% NZ demonstrated the greatest volume expansion of 43 ml and 28 ml, respectively. The control AAC showed a reduced expansion capacity, whereas the PG-replaced AACs displayed a larger expansion than the control. After one hundred minutes, the rate of volume expansion became stable. The volume expansion measurements of the paste are primarily regulated by two key factors: the aerating agent's gas generation potential and the AAC paste's stiffening. The relatively modest volume expansion of the control AAC is likely due to its high yield stress and low gas generation rate. Because of the high dose of PG and the amount of aluminium powder employed as an aerating agent, the yield stress of the AAC paste was significantly reduced, which led to a higher volume expansion. The correct coordination between the two components remains essential to produce an excellent cellular structure in AAC. This is because proper coordination between the two features is also necessary, in addition to the aerating agent's more extensive gas production measurements and the lower yield stress development rate of fresh AAC paste.

3.2. Effect of PG on AACs strength and density

3.2.1. Density measurements

When evaluating the qualities of AAC, bulk density is an essential element that is taken into consideration. **Figure 5** exemplifies by what means the proportions of PG and NZ affect the mixes of AAC concerning their dry densities. The density decreased from 741 g/cm^3 to 620 g/cm^3 at 10% NZ, while it decreased to 642 g/cm^3 at 20% NZ as the percentage of PG replacement increased from 0% to 20%.

The density was lowered by approximately 16.3% and 13.4% at 10% and 20% NZ, respectively, once fly ash was replaced with PG equal to 20% of the entire weight. The decrease in density with an increase in PG content can be explained by the formation of AFt and AFm during the pre-curing stage, which leads to a reduction in AAC density. This phenomenon can be detected when the PG concentration of the material is increased. The PG content in the sample significantly impacts the bulk density. The evolution of AFt and AFm has a bigger impact on the developed sample density than the negative effect that PG has on gas foaming. This is because PG harms gas foaming.

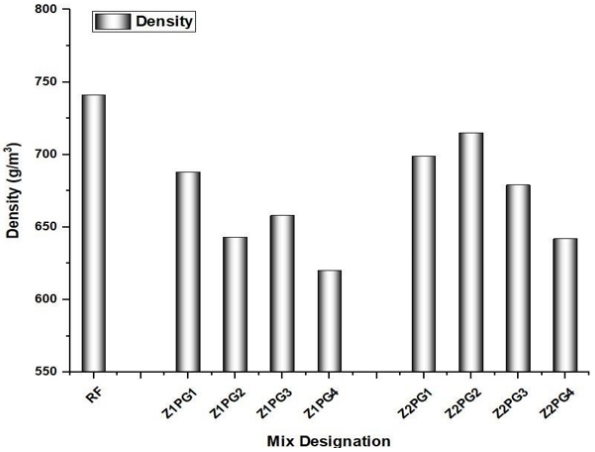

Figure 5. Effect of PG on the density of developed AACs

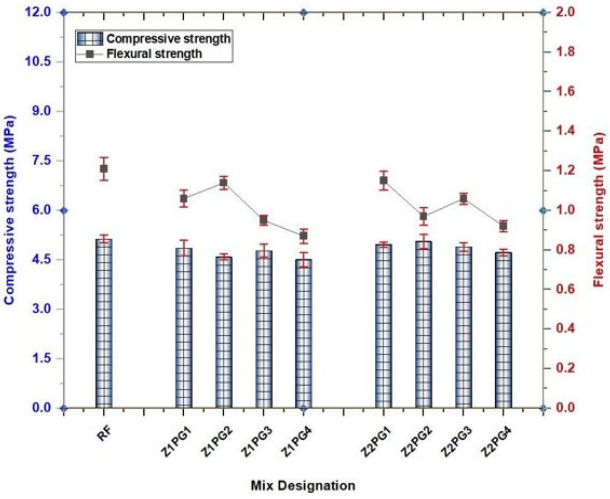

Figure 6. Effect of PG on the strength of developed AACs

3.3. Compressive strength

As shown in **Figure 6**, the compressive strength fell from 5.1 MPa to 4.5 MPa and 5.1 MPa to 4.7 MPa at 10% NZ and 20% NZ, respectively, as the percentage of PG replacement improved from 0% to 20%. Furthermore, the drop in AAC density can be linked to the compressive strength loss experienced by the material. It is common knowledge that compressive strength is directly proportional to bulk density. If the density of AAC is reduced, the material's compressive strength will often fall as a direct consequence, as this is a general rule. The decrease in compressive strength can also be partially attributed to the reduction in tobermorite and C-S-H. It is well-known that the formation of tobermorite and C-S-H under autoclave conditions can contribute to an increase in the strength of AAC. A higher proportion of PG results in greater gypsum in the AAC matrix. This, in turn, encourages the development of anhydrite while simultaneously reducing the development of tobermorite and C-S-H, ultimately reducing strength (Shekarchi *et al*., 2012). However, the strength of Z1PG3 improved somewhat when the proportion of RG replacement grasped 15% at 10% NZ, and a similar modest gain in strength can be perceived at 10% PG containing AAC (Z2PG2) in the compound. In the succeeding hydrothermal reaction, the synthesis of tobermorite and the occurrence of an adequate quantity of anhydrite jointly ensure the material's tensile strength.

3.3.1. Flexural strength

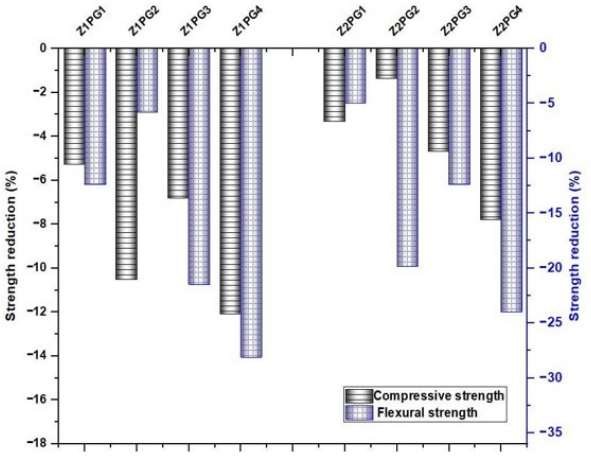

Figure 7. Strength reduction percentage of developed AACs

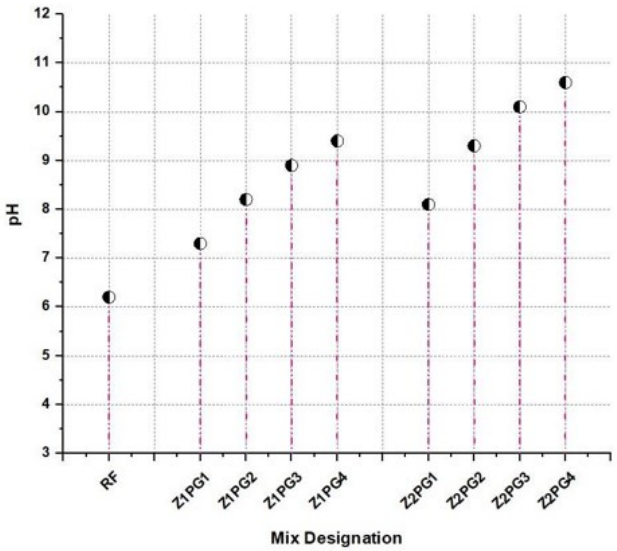

Figure 8. pH at an early phase of gas foaming

Compared to the control AAC that did not contain additives, the flexural strength was reduced by 28.1% at 10% NZ and 24% at 20% NZ. The result of 1.21 MPa was recorded as the control sample's flexural strength, the highest value obtained. However, the strength values showed a modest rise at particular percentages (10% PG at 10% NZ and 15% PG at 20% NZ), while it's true that the strength values overall had decreased. Compared to the control AAC, the flexural strength revealed a percentage drop of approximately 12.4, 5.8, 21.5, 28.1%, and 5, 19.8,

12.4, and 24.0 at 10 and 20% NZ, respectively. These numbers refer to the reduction in strength at 10 and 20% NZ. The percentages of strength reduction achieved by developed AACs are depicted in **Figure 7**.

3.4. Gas foaming rate

Figure 8 illustrates the impact of different dosages of PG on slurry behaviour. The control AAC had a pH value of 6.2, which indicates that the acidity level was relatively low. After the PG was added, it should not surprise that the slurry's pH level improved. To be more exact, the rise in the dose of PG from 5% to 20% caused the AAC slurry pH to rise from 7.3 to 9.4 and from 8.1 to 10.6 when the concentration of NZ was either 10% or 20%. Therefore, an efficient method for elevating the pH level of slurry is to combine the incorporation of PG with the employment of natural zeolite.

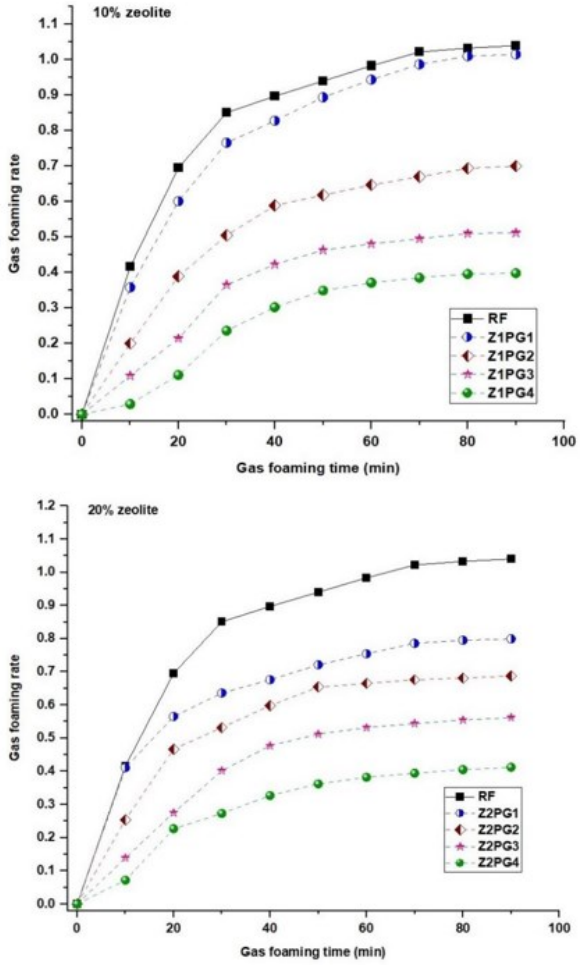

Figure 9. Gas foaming rate of AACs

It is evident from **Figure 9** that the quantity of PG used immediately impacts the volume of foam produced by the gas, predominantly in the first ten minutes. Within the first ten minutes, the gas foaming rate decreased as a straight effect of a reduction in the dosage of PG from 20% to 0%. This can most likely be attributed to the lower alkalinity that results from lowering PG. Due to the passivation layer already present on the aluminium powder surface, the early foaming response was stifled. As a result, there was no delay in the onset of the premature gas foaming response in AAC samples. It is clear that in the nonappearance of any PG component, the development of the slurry reached over 40 percent in the first 10 minutes. Along with this, the rapid rate of expansion that occurred during the initial stage also made it easier for the early slurry's strength to expand. Once the expansion rate of AAC exceeds its setting rate, it can cause hydrogen escape and collapse (Li *et al*., 2024). Despite the appropriate foaming of the control AAC in this study, the expansion rate within 10 minutes indicated significant potential risks in practical engineering applications.

3.5. Thermal conductivity

At a temperature of 194^{0}C inside the autoclave, **Figure 10** illustrates the thermal conductivity measurements of AAC that contain varying amounts of Phospho-Gypsum (PG) and Natural Zeolite (NZ). It is easy to see a connection between thermal and strength characteristics. In both sets of research, a growth in the compressive strength commanded towards an increment in the heat conductivity of the material. However, a modest rise in conductivity values is noticed when the PG level reaches 15% and 10% in AAC at 10% NZ and 20% NZ, respectively. The control AAC has the maximum thermal conductivity, and the values declined dramatically as the PG content increased. This agrees with the findings about the compressive behaviour of the created AACs.

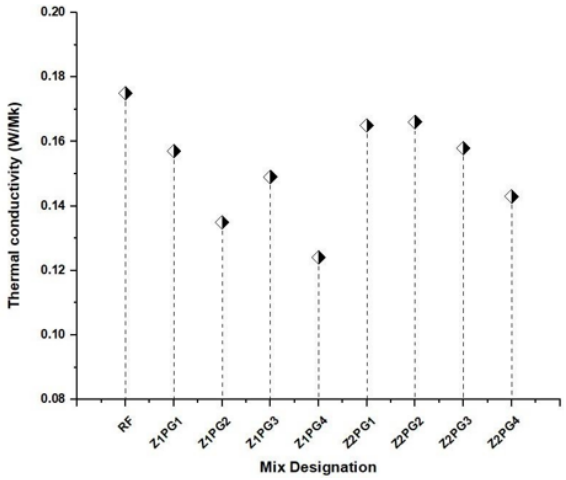

Figure 10. Effects of PG on the thermal conductivity of AAC

3.6. XRD analysis

An X-ray diffraction (XRD) analysis was conducted to confirm the phases formed with different levels of RG present in the AAC. The predominant minerals identified include tobermorite, mullite, anhydrite, katoite, calcite, and residual quartz, as depicted in **Figure 11**. The substitution with PG does not affect the mineral compositions; they are unaltered. On the other hand, the anhydrite, tobermorite, and katoite concentrations are entirely dissimilar. When PG is used in place of AAC, there is a considerable alteration in the mineral compositions of each mineral. Under high pressure and temperature conditions, an increased amount of anhydrite is produced because of the ongoing increase in PG replacement. As previously noted, an essential phase of Tobermorite gives AAC samples superior compressive strength while lowering their density (Sun *et al*., 2021; Chen *et al*., 2024).

It is abundantly evident that the substitution of PG does not affect the tobermorite, which serves as the primary result of the reaction. However, a minor shift matching the complicated structure of tobermorite is observed to occur in the peak locations of tobermorite when PG-AAC samples are analyzed. This change resulted in a slight shift in the peak positions of tobermorite. It has been proposed that incorporating waste by-products into AAC can alter the reaction products.

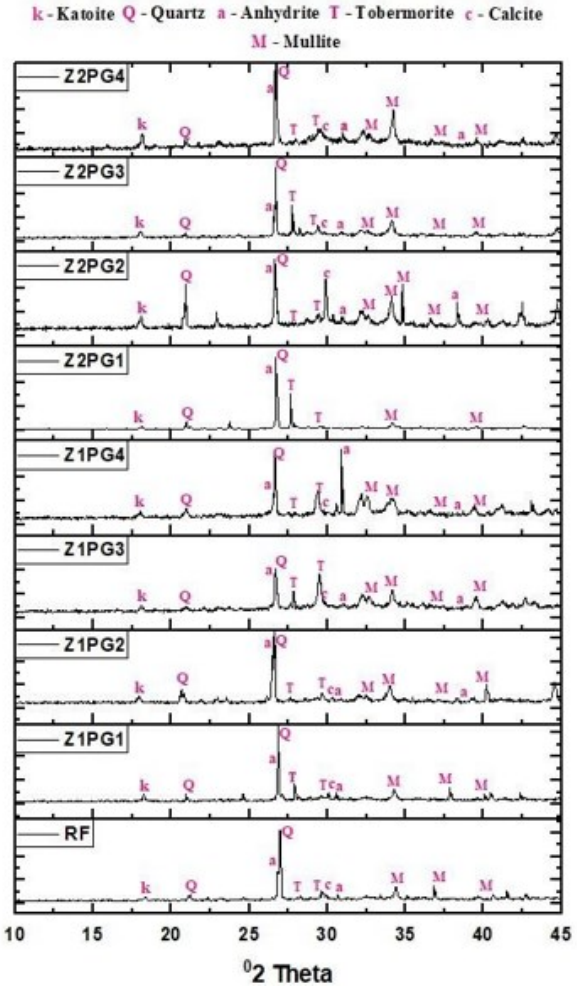

Figure 11. XRD patterns of developed AACs

3.7. FTIR analysis

The FTIR spectra of the AAC samples are characterized in **Figure 12**. The bending vibration band of molecule H_2O correlates to the absorption band located approximately 1643 cm^{-1} in wavelength. The stretching vibrations of the O–H group are accounted for by the absorption bands centered at 3445 cm^{-1} in H_2O, C-S-H, C–H, and tobermorite. The advancement of hydrogen bonding, which may take on various strengths, is responsible for broadening the band. The peaks that may be found in the range of 1429 cm^{-1} to 1450 cm^{-1} are the asymmetric stretching vibration peaks of CO_3^{2-}, and their presence indicates that calcium carbonate is present in the sample. It is conceivable that this happened due to the carbonization of CO_2 that grabbed the place throughout the sample preparation and drying processes. The absorption bands with the greatest strength can be evident in the region of 1100 cm^{-1}. These bands are associated with the asymmetrical stretching vibrations of SiO_4 tetrahedra, with peaks at approximately 690, 790, and 807 cm^{-1} corresponding to the bending vibrations of Si-O-Si. The band at 470 cm^{-1} is attributed to O-Si-O deformation or bending modes.

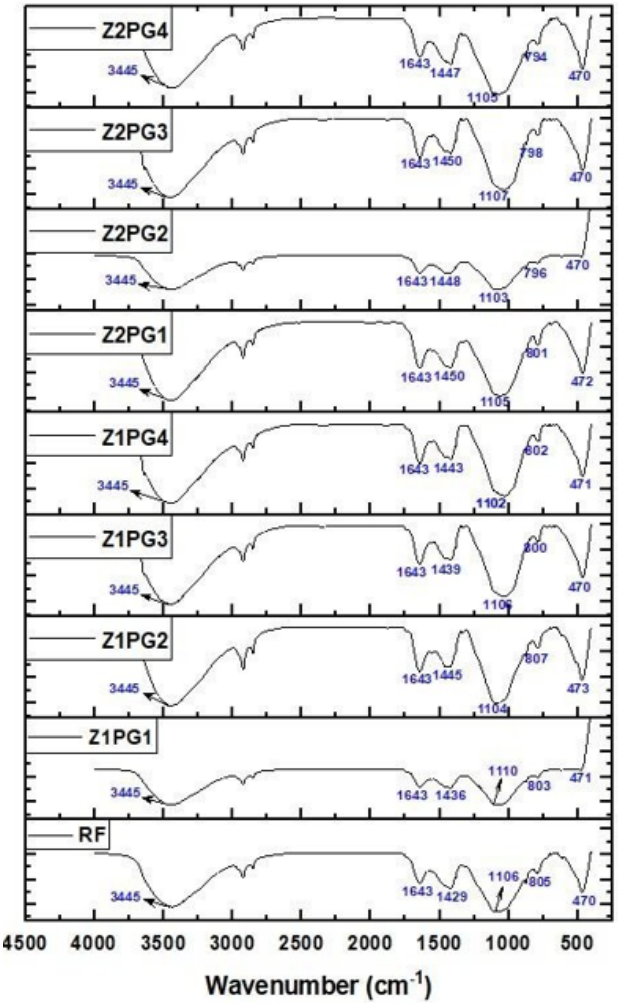

Figure 12. FTIR patterns of developed AACs

4. Leaching potential and associated risks for each material

4.1. Natural zeolite

Natural zeolites are generally considered environmentally friendly; however, they can still leach trace amounts of heavy metals, depending on their source and composition. Studies have shown that while zeolites can absorb pollutants, they may also release certain contaminants under specific conditions, such as acidic environments (Tran *et al*., 2019). Therefore, careful sourcing and testing are necessary to minimize the risk of leaching.

4.2. Aluminum powder

Aluminum powder can lead to leaching of aluminum ions, particularly in alkaline environments, which can be toxic to aquatic life if released into water bodies (Mahedi *et al*., 2019). The leaching potential increases with the particle size and surface area of aluminum powder. Moreover, when aluminum is exposed to moisture, it may undergo

oxidation, producing hydrogen gas, which can pose additional safety hazards.

4.3. Phosphogypsum

Phosphogypsum, a by-product of phosphate fertilizer production, has raised significant environmental concerns due to its potential to leach harmful substances, including heavy metals and radioactive elements (Chernysh *et al*., 2021). Studies have shown that when phosphogypsum is not properly stabilized or contained, it can leach these contaminants into surrounding soils and waterways, posing risks to both human health and the environment.

4.4. Mitigation strategies

To mitigate the risks of leaching and pollution:

- **Monitoring and testing**: Regular leachate testing should be conducted to monitor for heavy metals and other contaminants.
- **Material stabilization**: Techniques such as encapsulation and optimizing mix designs can help stabilize contaminants within construction materials.
- **Controlled use**: Ensuring that materials are sourced from reputable suppliers and are free from significant contaminants can also reduce leaching risks.

5. Limitations and disadvantages

5.1. Performance limitations

- **Mechanical properties**: While using these materials may enhance certain properties, such as thermal conductivity, they may not achieve the same mechanical strength as conventional concrete components. Research indicates that the incorporation of alternative materials can sometimes lead to a reduction in compressive strength, especially if not optimally blended.
- **Durability issues**: The long-term durability of AAC containing these materials may be a concern. Natural zeolite, while beneficial for some properties, can have varying pozzolanic activity based on its origin, potentially leading to inconsistent performance in different environments.

5.2. Environmental concerns

- **Leaching potential**: As discussed previously, materials like phosphogypsum can leach heavy metals and other contaminants into the environment if not properly managed (Mäkitie et al., 2019). This raises concerns about the sustainability of using such materials in construction, as they may pose risks to both human health and ecosystems.
- **Resource availability**: The availability and sourcing of these materials may also present challenges. For example, while natural zeolite is abundant in some regions, it may not be as readily available in others, leading to increased transportation emissions and costs.

5.3. Economic considerations

- **Cost implications**: The economic feasibility of utilizing these alternative materials can be a significant drawback. Although they may be cheaper than traditional materials in some contexts, processing, transportation, and potential treatment costs associated with leachate management can offset initial savings.
- **Market acceptance**: The construction industry is often slow to adopt new materials due to established standards and practices. Gaining acceptance for AAC incorporating these materials may require extensive testing and validation, which could delay their implementation.

5.4. Regulatory challenges

- **Standards and guidelines**: There may be a lack of established regulatory frameworks governing the use of alternative materials in construction, particularly for by-products like phosphogypsum. This could lead to complications in compliance with building codes and regulations.

While the incorporation of natural zeolite, aluminum powder, and phosphogypsum in AAC offers potential benefits, it is essential to consider these limitations and disadvantages in the context of sustainable construction practices. Addressing these concerns will require ongoing research and innovation to optimize material formulations and ensure environmental safety.

6. Conclusions

The study showed several outcomes that can be summarized as follows:

The incorporation of PG into AAC has the potential to reduce its workability. This could be because PG has a smaller particle size and a greater specific surface area than AAC, meaning it can absorb more water. Due to the slurry's weak fluidity and rapid thickening, it had poor gas generation; as a result, the pores tended to form horizontally and had improved interconnectivity.

The yield stress of the control AAC paste was the highest at any given time, followed by rising PG-containing AACs, and then the yield stress was at its lowest for the 20% PG-substituted AAC. Because of its high yield stress and low gas generation rate, control AAC exhibits the most minor volume expansion possible. Because of employing a substantial dosage of PG in conjunction with a proportion of aluminium powder as an aerating agent, the yield stress of the AAC paste was suggestively condensed, which directed to a bigger volume expansion.

Using PG in place of fly ash can potentially lessen the density of the sample in both the 10% and 20% NZ substituted AACs. Even if using PG instead of fly ash successfully lowered the rate of gas foaming, the creation of AFt and AFm as a product of this process can cause the density of the sample to drop by a lot.

The loss in compressive and flexural strength is attributable to the drop in density of the AAC due to increasing the percentage of PG replacement from 0% to

20% in the material. Growth in the proportion of PG results in a higher proportion of gypsum being present in the AAC reaction matrix; this, in turn, encourages the creation of anhydrite; this, in turn, leads to a lessening in the proportions of tobermorite and C-S-H; and, ultimately, this results in a weaker composite.

To be more exact, the value of the AAC slurry's pH rose as the proportion of PG in the mixture climbed from 5% to 20%. The quantity of PG used immediately impacts how much foam the gas produces, particularly in the first ten minutes. In the first ten minutes after the PG dosage was cut from 20% to 0%, there was a drop in the rate at which the gas foamed. The occurrence of the passivation layer on the aluminium powder surface was accountable for preventing an early foaming response from occurring.

The AAC made using phosphogypsum exhibited satisfactory strength, density, and thermal conductivity results. The control AAC had maximum thermal conductivity, whereas the values declined dramatically as the PG level increased. However, a modest rise in conductivity values was found when the PG content reached 15% and 10% in AAC at 10% NZ and 20% NZ, respectively.

Before autoclaving, C-S-H gels and CH had already been created, and after autoclaving, the majority of the C-S-H gels had been altered into tobermorite. Tobermorite, which is the primary result of the reaction, is not affected in any way by the PG substitution, as can be seen. However, the peak positions of tobermorite are seen to alter ever-so-slightly when PG-AAC samples are analysed, and this shift is seen to correspond to the complicated structure of tobermorite. It has been concluded that including waste by-products in AAC can change the reaction products.

References

Ahmed H., Khan S. and Niazi M. (2024). Enhancing the properties of aerated concrete with natural zeolites. *Materials Science Forum*, **1052**, 123–132. https://doi.org/10.4028/www.scientific.net/MSF.1052.123.

Ahmed S., Zhang W. and Liu H. (2022). Eco-friendly autoclaved aerated concrete with improved thermal performance. *Journal of Cleaner Production*, **364**, 132764. https://doi.org/10.1016/j.jclepro.2022.132764.

Alexa-Stratulat S.M., Olteanu I., Toma A.M., Pastia C., Banu O.M., Corbu O.C. and Toma I.O. (2023). The Use of Natural Zeolites in Cement-Based Construction Materials—A State of the Art Review. *Coatings*, ***14***(1): 18. https://doi.org/10.3390/coatings14010018

Aminul H., Chen M.B., Liu Y., Farasat Ali Shah S. and Ahmad M.R. (2020). Improvement of physico-mechanical and microstructural properties of magnesium phosphate cement composites comprising with Phosphogypsum. *Journal of Cleaner Production* **261**: 121268. https://doi.org/10.1016/j.jclepro.2020.121268.

Arunprathap K.U., Gokuldeepan P. and Sunilaa George (2022). Effect of By-product Phosphogypsum in Fly-ash Incorporated Concrete. *International Journal of Creative Research Thoughts* (IJCRT), **10**(7): 67–78. https://ijcrt.org/papers/IJCRT2207666.pdf

Asadi I., Shafigh Abu Hassan Z.F.B. and Mahyuddin N.B. (2018). Thermal conductivity of concrete – A review. *Journal of Building Engineering* 20: 81–93. https://doi.org/10.1016/j.jobe.2018.07.002.

ASTM C1693-11 (2017). Standard Specification for Autoclaved Aerated Concrete (AAC), *American Society of Testing and Materials*, USA. https://doi.org/10.1520/c1693-09e01.

ASTM C471M-20 (2024). Standard Test Methods for Chemical Analysis of Gypsum and Gypsum Products (Metric), *American Society of Testing and M*aterials, USA. https://doi.org/10.1520/c0471m-17.

Cai L., Li X., Ma B. and Lv Y. (2018). Effect of binding materials on carbide slag based high utilization solid-wastes autoclaved aerated concrete (HUS-AAC): Slurry, physic- mechanical property and hydration products. *Construction and Building Materials* **188**: 221–236. https://doi.org/10.1016/j.conbuildmat.2018.08.115.

Campos M.P., Costa L.J.P., Nisti M.B. and Mazzilli B.P. (2017). Phosphogypsum recycling in the building materials industry: assessment of the radon exhalation rate. *Journal of Environmental Radioactivity*, **172**, 232–236. https://doi.org/10.1016/j.jenvrad.2017.04.002.

Chen G., Li F., Jing P., Geng J. and Si Z. (2021) Effect of Pore Structure on Thermal Conductivity and Mechanical Properties of Autoclaved Aerated Concrete. *Materials* **14**. https://doi.org/10.3390/ma14020339.

Chen W., Yang F. and Xu Q. (2024). Utilization of phosphogypsum in building materials: A comprehensive review. *Construction and Building Materials*, **356**, 129278. https://doi.org/10.1016/j.conbuildmat.2023.129278.

Chernysh Y., Yakhnenko O., Chubur V. and Roubík H. (2021). Phosphogypsum recycling: a review of environmental issues, current trends, and prospects. *Applied Sciences*, **11**(4): 1575. https://doi.org/10.3390/app11041575

Cong X.Y., Lu S., Yao Y. and Wang Z. (2016). Fabrication and characterization of self-ignition coal gangue autoclaved aerated concrete. *Materials & Design* **97**, 155–162. https://doi.org/10.1016/j.matdes.2016.02.068.

El-Didamony H., Amer A., Mohammed M. and El-Hakim M. (2019). Fabrication and properties of autoclaved aerated concrete containing agriculture and industrial solid wastes. *Journal of Building Engineering* **22**. https://doi.org/10.1016/j.jobe.2019.01.023.

Falliano D., Parmigiani S., Suarez-Riera D., Ferro G.A. and Restuccia L. (2022). Stability, flexural behavior and compressive strength of ultra-lightweight fiber-reinforced foamed concrete with dry density lower than 100 kg/m3. *Journal of Building Engineering* **51**: 104329. https://doi.org/10.1016/j.jobe.2022.104329.

González-Torres M., Pérez-Lombard L., Coronel J.F., Maestre I.R. and Yan D. (2022). A review on buildings energy information: Trends, end-uses, fuels and drivers. *Energy Reports* **8**: 626–637. https://doi.org/10.1016/j.egyr.2021.11.280.

Guo X. and Zhang T. (2020). Utilization of municipal solid waste incineration fly ash to produce autoclaved and modified wall blocks. *Journal of Cleaner Production* **252**: 119759. https://doi.org/10.1016/j.jclepro.2019.119759.

He J., Gao Q., Song X., Bu X. and He J. (2019). Effect of foaming agent on physical and mechanical properties of alkali-activated slag foamed concrete. *Construction and Building*

Materials **226**: 280–287. https://doi.org/10.1016/j.conbuildmat.2019.07.302.

Holanda F.d.C., Schmidt H. and Quarcioni V.A. (2017). Influence of phosphorus from phosphogypsum on the initial hydration of Portland cement in the presence of superplasticizers. *Cement and Concrete Composites* **83**: 384–393. https://doi.org/10.1016/j.cemconcomp.2017.07.029.

Huang F., Zhang J., Zheng X., Wu Y., Fu T., Easa S., Liu W. and Qiu R. (2022). Preparation and performance of autoclaved aerated concrete reinforced by dopamine- modified polyethylene terephthalate waste fibers. *Construction and Building Materials* **348**: 128649. DOI: https://doi.org/10.1016/j.conbuildmat.2022.128649.

IS 12269 (1987). 53 grade ordinary Portland cement, Indian Standards, India. https://doi.org/10.3403/30304852.

Johnson R., Hall D. and Wang M. (2021). Mechanical behavior of AAC blocks with natural zeolite additives. *Journal of Construction Engineering and Management*, **147**(12), 04021195. https://doi.org/10.1061/(ASCE)CO.1943-7862.0002178.

Kadhim A., Sadique M., Al-Mufti R. and Hashim K. (2020). Long-term performance of novel high-calcium one-part alkali-activated cement developed from thermally activated lime kiln dust. *Journal of Building Engineering* **32**: 101766. https://doi.org/10.1016/j.jobe.2020.101766.

Kim H., Hong J. and Pyo S. (2018). Acoustic characteristics of sound absorbable high performance concrete. *Applied Acoustics* **138**: 171–178. https://doi.org/10.1016/j.apacoust.2018.04.002.

Koudelka T., Kruis J. and Maděra J. (2015). Coupled shrinkage and damage analysis of autoclaved aerated concrete. *Applied Mathematics and Computation* **267**, 427–435. https://doi.org/10.1016/j.amc.2015.02.016.

Kumar P., Patel R. and Reddy B. (2024). Thermal insulation performance of autoclaved aerated concrete with recycled materials. *Energy and Buildings*, **274**, 112375. https://doi.org/10.1016/j.enbuild.2023.112375.

Laad D. and Jatti V. (2015). Investigation into the effect of Aluminium powder on Mechanical, Tribological and Electrical properties of Al-ABS composites. *WSEAS Transactions on Applied and Theoretical Mechanics*, E-ISSN: 2224–3429 10: 47–53.

Li M., van Keulen W., Tijs E., Ven V.D M. and Molenaar A. (2015). Sound absorption measurement of road surface with in situ technology. *Applied Acoustics* **88**: 12–21. https://doi.org/10.1016/j.apacoust.2014.07.009.

Li Q., Li K., Ni W., Zhang S., Li D. and Chen W. (2019). Analysis on Gold Tailings- Based Aerated Concrete in Different Phases of Autoclave Curing Based on Nuclear Magnetic Resonance. *Revue des composites et des matériaux avancés* **29**: 381–387. https://doi.org/10.18280/rcma.290607.

Li W., Zhang C. and Zhou X. (2020). Investigation of AAC with phosphogypsum and natural zeolite. *Journal of Sustainable Cement-Based Materials*, **9**(4), 255–272. https://doi.org/10.1080/21650373.2020.1767742.

Li X., Zhang Y., Wang H. and Gao M. (2024). Mechanical and thermal properties of zeolite-based autoclaved aerated concrete. *Journal of Building Engineering*, **50**, 104587. https://doi.org/10.1016/j.jobe.2024.104587.

Liu Y., Chen G., Wang Z., Chen Z., Gao Y. and Li F. (2020). On the Seismic Performance of Autoclaved Aerated Concrete Self-Insulation Block Walls. *Materials* **13**. https://doi.org/10.3390/ma13132942.

Loginova E., Schollbach K., Proskurnin M. and Brouwers H.J.H. (2023). Mechanical performance and microstructural properties of cement mortars containing MSWI BA as a minor additional constituent. *Case Studies in Construction Materials* **18**: e01701. https://doi.org/10.1016/j.cscm.2022.e01701.

Ma B.G., Cai L.X., Li X.G. and Jian S.W. (2016). Utilization of Iron Tailings as Substitute in Autoclaved Aerated Concrete: Physico-mechanical and Microstructure of Hydration Products. *Journal of Cleaner Production* **127**. https://doi.org/10.1016/j.jclepro.2016.03.172.

Mahedi M., Cetin B. and Dayioglu A.Y. (2019). Leaching behavior of aluminum, copper, iron and zinc from cement activated fly ash and slag stabilized soils. *Waste Management*, **95**: 334–355. https://doi.org/10.1016/j.wasman.2019.06.018

Miao C., Wang H. and Liu X. (2023). Enhanced mechanical properties of aerated concrete with natural zeolite. *Construction and Building Materials*, **340**, 127835. https://doi.org/10.1016/j.conbuildmat.2023.127835.

Mohammadi M., Fakharian P. and Nemati A. (2020). Influence of natural zeolites on the mechanical properties of AAC. *Journal of Building Engineering*, **32**, 101730. https://doi.org/10.1016/j.jobe.2020.101730.

Murali G. and Azab M. (2023). Recent research in utilization of phosphogypsum as building materials. *Journal of Materials Research and Technology*, **25**: 960–987. https://doi.org/10.1016/j.jmrt.2023.05.272

Nambiar E., Ramachandran D. and Menon V. (2023). Thermal performance of phase change material-coated AAC with recycled content. *Sustainability*, **15**(1), 187. https://doi.org/10.3390/su15010187.

Natarajan R., Priya P. and Ravikumar V. (2021). Recycling of waste materials in AAC: A sustainable approach. *Sustainability*, **13**(24), 13927. https://doi.org/10.3390/su132413927.

Pinilla Melo J., Sepulcre Aguilar A. and Hernández Olivares F. (2014). Rheological properties of aerated cement pastes with fly ash, metakaolin and sepiolite additions. *Construction and Building Materials* **65**: 566–573. https://doi.org/10.1016/j.conbuildmat.2014.05.034.

Qian B. and Hu Y. (2023). The influence of disused ZSM-5 on the performance of phosphogypsum-based autoclaved aerated concrete. *Buildings*, **13**(12), 3012. https://doi.org/10.3390/buildings13123012.

Qiao Y., Zhang H. and Wang R. (2020). Sustainable construction materials: Phosphogypsum and zeolite in AAC. *Construction and Building Materials*, **243**, 118304. https://doi.org/10.1016/j.conbuildmat.2020.118304.

Qu X. and Zhao X. (2017). Previous and present investigations on the components, microstructure and main properties of autoclaved aerated concrete – A review. *Construction and Building Materials* **135**: 505–516. https://doi.org/10.1016/j.conbuildmat.2016.12.208.

Rahman R.A., Fazlizan A., Asim N. and Thongtha A. (2021). A review on the utilization of waste material for autoclaved aerated concrete production. *Journal of Renewable Materials*, **9**(1): 61–72. https://doi.org/10.32604/jrm.2021.013296

Rashad A.M. (2017). Phosphogypsum as a construction material. *Journal of Cleaner Production* **166**, 732–743. https://doi.org/10.1016/j.jclepro.2017.08.049.

Reddy B.V., Prasad D. and Gupta A. (2022). Utilizing waste materials in the production of autoclaved aerated concrete. *Journal of Building Engineering*, **45**, 103509. https://doi.org/10.1016/j.jobe.2022.103509.

Revilla-Cuesta V., Faleschini F., Zanini M.A., Skaf M. and V. Ortega-López (2021). Porosity-based models for estimating the mechanical properties of self-compacting concrete with coarse and fine recycled concrete aggregate. *Journal of Building Engineering* **44**: 103425. https://doi.org/10.1016/j.jobe.2021.103425.

Rosales J., Pérez S.M., Cabrera M., Gázquez M.J., Bolivar J.P., de Brito J. and Agrela F. (2020). Treated phosphogypsum as an alternative set regulator and mineral addition in cement production. *Journal of Cleaner Production* **244**: 118752. https://doi.org/10.1016/j.jclepro.2019.118752.

Shekarchi M., Ahmadi B. and Najimi M. (2012). Use of natural zeolite as pozzolanic material in cement and concrete composites. Chapter, **27**, 665–694. https://doi.org/10.2174/978160805261511201010665

Shekarchi M., Ahmadi B., Azarhomayun F., Shafei B. and Kioumarsi M. (2023). Natural zeolite as a supplementary cementitious material–A holistic review of main properties and applications. *Construction and Building Materials*, **409**: 133766. https://doi.org/10.1016/j.conbuildmat.2023.133766

Schreiner J., Jansen D., Ectors D., Goetz-Neunhoeffer F., Neubauer J. and Volkmann S. (2018). New analytical possibilities for monitoring the phase development during the production of autoclaved aerated concrete. *Cement and Concrete Research* **107**: 247–252. https://doi.org/10.1016/j.cemconres.2018.02.028.

Seddighi F., Pachideh G. and Salimbahrami S.B. (2021). A study of mechanical and microstructures properties of autoclaved aerated concrete containing nano-graphene. *Journal of Building Engineering* **43**: 103106. https://doi.org/10.1016/j.jobe.2021.103106.

Serhat Baspinar M., Demir I., Kahraman E. and Gorhan G. (2014). Utilization potential of fly ash together with silica fume in autoclaved aerated concrete production. *KSCE Journal of Civil Engineering* **18**(1): 47–52. https://doi.org/10.1007/s12205-014-0392-7.

Singh K., Kumar A. and Gupta R. (2020). Thermal and mechanical analysis of AAC with waste by-products. *Journal of Cleaner Production*, **273**, 122923. https://doi.org/10.1016/j.jclepro.2020.122923.

Suchorab Z., Barnat-Hunek D., Franus M. and Łagód G. (2016) Mechanical and Physical Properties of Hydrophobized Lightweight Aggregate Concrete with Sewage Sludge. *Materials* **9**. https://doi.org/10.3390/ma9050317.

Sun Y., Li X. and Zhang H. (2021). Thermal and mechanical properties of zeolite-phosphogypsum aerated *concrete. Construction and Building Materials*, **307**, 124945. https://doi.org/10.1016/j.conbuildmat.2021.124945.

Tian T., Yan Y., Hu Z., Xu Y., Chen Y. and Shi J. (2016). Utilization of original phosphogypsum for the preparation of foam concrete. *Construction and Building Materials* **115**, 143–152. https://doi.org/10.1016/j.conbuildmat.2016.04.028.

Tran Y.T., Lee J., Kumar P., Kim K.H. and Lee S.S. (2019). Natural zeolite and its application in concrete composite production. *Composites Part B: Engineering*, **165**, 354–364. https://doi.org/10.1016/j.compositesb.2018.12.084

Trindade A.D., Coelho G.B.A. and Henriques F.M.A. (2021). Influence of the climatic conditions on the hygrothermal performance of autoclaved aerated concrete masonry walls *Journal of Building Engineering* **33**, 101578. https://doi.org/10.1016/j.jobe.2020.101578.

Walczak P., Szymański P. and Różycka A. (2015). Autoclaved Aerated Concrete based on Fly Ash in Density 350kg/m3 as an Environmentally Friendly Material for Energy–Efficient Constructions. *Procedia Engineering* **122**, 39–46. https://doi.org/10.1016/j.proeng.2015.10.005.

Wang Y., Wang W., Wang D., Liu Y. and Liu J. (2021). Study on the influence of sample size and test conditions on the capillary water absorption coefficient of porous building materials. *Journal of Building Engineering* **43**, 103120. https://doi.org/10.1016/j.jobe.2021.103120.

Wang J., Li S. and Zhou Y. (2023). Optimization of phosphogypsum and zeolite mixtures in aerated concrete. *Journal of Cleaner Production*, **398**, 136445. https://doi.org/10.1016/j.jclepro.2023.136445.

Xu C., Nehdi M.L., Wang K. and Guo Y. (2021). Experimental study on seismic behavior of novel AAC prefabricated panel walls. *Journal of Building Engineering* **44**: 103390. https://doi.org/10.1016/j.jobe.2021.103390.

Yang S., Yao X., Li J., Wang X., Zhang C., Wu S., Wang K. and Wang W. (2021). Preparation and properties of ready-to-use low-density foamed concrete derived from industrial solid wastes. *Construction and Building Materials* **287,** 122946. https://doi.org/10.1016/j.conbuildmat.2021.122946.

Yuan B., Straub C., Segers S., Q. L. Yu and H. J. H. Brouwers (2017). Sodium carbonate activated slag as cement replacement in autoclaved aerated concrete. *Ceramics International* **43**(8): 6039-6047. https://doi.org/10.1016/j.ceramint.2017.01.144.

Zhai S., Zhang P., Xian Y., Zeng J. and Shi B. (2018). Effective thermal conductivity of polymer composites: Theoretical models and simulation models. *International Journal of Heat and Mass Transfer* **117**, 358–374. https://doi.org/10.1016/j.ijheatmasstransfer.2017.09.067.

Zhang X., Liu Y. and Wang J. (2022). Thermal insulation properties of AAC incorporating industrial by-products. *Construction and Building Materials*, **330**, 127252. https://doi.org/10.1016/j.conbuildmat.2022.127252.

Zhang Y., Zhang S., Zhao W., Jiang X., Chen Y., Hou J., Wang Y., Yan Z. and Zhu H. (2023). Influence of multi-scale fiber on residual compressive properties of a novel rubberized concrete subjected to elevated temperatures. *Journal of Building Engineering* **65**, 105750. https://doi.org/10.1016/j.jobe.2022.105750.

Zhao F., Li X. and Zhang Z. (2020). Optimization of autoclaved aerated concrete mixtures with natural zeolites. *Materials Science and Engineering: A*, **788**, 139574. https://doi.org/10.1016/j.msea.2020.139574.

Zhao X., Zhang L. and Chen H. (2023). Sustainable use of industrial waste in construction materials: A review. Resources, *Conservation and Recycling*, **190**, 106735. https://doi.org/10.1016/j.resconrec.2023.106735.